

# Effects of intermetallic formation at the interface between copper and lead-tin solder

J. O. G. PARENT, D. D. L. CHUNG\*, I. M. BERNSTEIN†

*Department of Metallurgical Engineering and Materials Science, Carnegie Mellon University, Pittsburgh, Pennsylvania 15213, USA*

An investigation was undertaken of the role of intermetallics in determining the strength of soldered joints, using copper and a lead-tin solder as the materials of interest. Joints formed at various times and temperatures were tested in shear, and measurements of the thickness of the two intervening intermetallic layers formed were taken. The temperature of formation was found to have the greatest effect on the strength, with the strength decreasing as the temperature increased. Failure at the interface occurred in two stages. In all cases, the first stage consisted of fracture within the intermetallic layer, accounting for partial separation of the interface only. The area of the interface showing this kind of behaviour increased with both time and temperature. Final stages of failure involved shear within the solder immediately above the intermetallic layers. The two intermetallic phases found at the interface were determined by X-ray diffraction to be  $\text{Cu}_6\text{Sn}_5$  and  $\text{Cu}_3\text{Sn}$ . Both intermetallics were found for all joint-forming conditions investigated. The growth of  $\text{Cu}_6\text{Sn}_5$  reached a limiting value for times longer than 30 min, but increased in thickness with temperature.  $\text{Cu}_3\text{Sn}$  also increased in thickness with temperature, but showed linear increases with time; the rate of increase was greater for the higher temperatures.

## 1. Introduction

Soft-soldering provides an inexpensive, reliable and relatively low-temperature means of joining two pieces of metal. This latter feature has made this technique especially valuable in the electronics industry, where exposure to high temperature could disrupt the increasingly complex circuits. The most commonly used soldering systems are those based on alloys of lead and tin, due to their low melting temperatures and excellent wetting properties. The reliability of these joints has always been of concern, especially as the formation of invariably brittle intermetallic compounds between the solder and the base metal has been observed in many cases. Several efforts have been made to study the formation of these compounds, though these studies have been limited and in some ways contradictory [1-9].

Establishing the identity and structure of the compounds formed is of importance in assessing possible effects on joint reliability. For the metals most commonly used in electronic applications (copper, nickel, silver, gold, palladium), consideration of the requisite phase diagrams with tin and lead [10] indicates that the possibility for compound formation exists primarily for tin. The role of lead in most solder systems is limited to that of a diluent, as noted by Thwaites [11] and confirmed in a number of studies. From X-ray analysis of reactions between copper and

tin or tin-bearing solders, Tu [6] and Dehaven *et al.* [7] confirmed that the intermetallics formed were exactly those predicted from the equilibrium phase diagram. Others have also demonstrated the presence of intermetallics of silver, gold, nickel, and palladium with tin [5, 8, 9] during reactions with molten solders. For metal-solder reactions in which the solder contains an appreciable amount of tin, it is therefore expected that the intermetallics formed will be complex compounds of the metal and tin.

The brittle nature of these compounds, as confirmed by Reicheneker [12] for the case of copper and tin, suggests that they should reduce the strength of the joint. Determination of the effect of intermetallic thickness on the strength of soldered joints in a variety of systems has been undertaken previously [1-3] with the general observation that the strength decreases with increasing amounts of intermetallic at the interface. These tests have, however, concentrated on examining the strength of the overall joint, and not the strength of the interface itself. Thus the results obtained represent the stress required to achieve separation at the weakest point in the joint, with fracture occurring at the solder/intermetallic interface. The stress values obtained were, not unexpectedly, of the same order of magnitude as tests performed on the solder itself [1, 2]. Failure within the intermetallic layer has been observed in very few cases [3], and only for

\* Present address: Department of Mechanical and Aerospace Engineering, State University of New York, Buffalo, New York, 14260, USA.

† Present address: Illinois Institute of Technology, Chicago, Illinois 60616, USA.

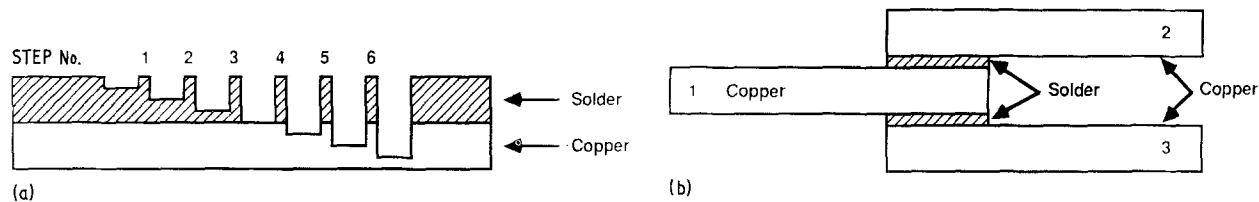


Figure 1 Final sample configurations for (a) bond strength determinations, and (b) X-ray examinations.

significant thicknesses of the intermetallic layer (greater than  $10\ \mu\text{m}$ ). These analyses for the effect of the intermetallic have remained largely empirical, however, and a clear understanding of the role of the intermetallics is not yet available.

Determination of the growth kinetics of the intermetallic layers has been attempted in a variety of different manners with some contradictory results. Hagstrom and Wild [1], using direct measurement of the intermetallic layer, obtained results indicating that growth was parabolic with time for short times, but reached a limiting value for times greater than 10 min. Muckett *et al.* [4], using similar measurements, suggested that the growth should be linear with time. In both cases, however, the individual phases making up the intermetallic layer were not considered independently, and there was no attempt to examine the interaction between the phases. Indirect measurement techniques have also been employed to determine the kinetics. Tu and Thompson [13], using Raman spectroscopy, found that  $\text{Cu}_6\text{Sn}_5$  grew linearly with time, and that  $\text{Cu}_3\text{Sn}$ , growing at the expense of the  $\text{Cu}_6\text{Sn}_5$ , progressed in a parabolic manner. DeHaven [14], employing *in situ* X-ray measurements, found that although  $\text{Cu}_6\text{Sn}_5$  initially grew linearly with time, after a period of time it followed a parabolic curve. In this case, the  $\text{Cu}_3\text{Sn}$  was not considered, and the results for the  $\text{Cu}_6\text{Sn}_5$  were based on measurements of the rate of decrease of the intensity of a copper peak, something which would be affected by the presence of an intermetallic other than the one of interest. The manner in which the intermetallics form is another area in which further understanding is required.

The aim of this work is to provide additional information about the effect of intermetallics on the strength of the bond between copper and a lead-tin solder. Primary interest is focused on the changes in strength with time and temperature, as well as establishing the changes in thickness as a function of these variables. X-ray diffraction experiments provide accurate identification of the phases present as well as documentation of their formation with time and temperature.

## 2. Experimental details

The experiments were divided into two major areas: mechanical testing and structure examination by X-rays. In both cases, the materials used were the same, with slightly different methods for sample preparation used for each. The base metal was a commercially prepared polycrystalline copper sheet of 99.95% purity, nominally 1.63 mm thick. A 63/37 Sn/Pb commercial solder alloy was used, along with a

proprietary acid flux. All heat treatments and testing were carried out in air.

For the mechanical tests, solder was melted in glass boats in a furnace controlled to  $\pm 2^\circ\text{C}$ . This arrangement provided a reservoir of solder sufficient to ensure a near constant bulk solder composition over the longest treatment times. The copper was prepared by first cutting it into strips 129.5 mm by 15.2 mm. These were then ground to 600 grit, cleaned and immersed in aqua regia (3 parts HCl, 1 part  $\text{HNO}_3$ ) for approximately 30 sec. The copper was then dried and fluxed, and placed in a furnace at  $150^\circ\text{C}$  for 30 min to drive off any water present in the flux. Following this, the strips were immersed (flux side down) in the solder, care being taken to minimize the formation of gas pockets at the interface. After treatment, the entire assembly was allowed to cool in air. Treatment temperatures were 230, 300 and  $350^\circ\text{C}$  and the times ranged from 30 to 180 min, at 30 min intervals. For each combination of time and temperature, the number of samples used was seven. Previous work by Tomlinson and Bryan [3] had indicated that statistically significant changes in the strength of joints formed with the aid of an inorganic acid flux could be measured if a sample number of ten was employed. Blickensderfer and Burrus [15] demonstrated, however, that a multi-step shear test, such as that used here, affords greater precision than previously used methods for investigating interfacial bond strength. Based on this fact, the sample number was reduced to seven in these experiments. Two samples were also prepared at 5 min for each temperature to provide an initial value of the bond strength for establishing changes in the values with time. Following heat treatment, the samples were machined to achieve the final configuration shown in Fig. 1a. The samples were nominally 4.57 mm thick, 127 mm long and 12.7 mm wide, although variations of 0.5 mm in the width were tolerated. The steps themselves were separated by a slot 9.57 mm wide, and the step width was kept constant at 1.27 mm. The steps were cut such that the fourth (see Fig. 1a) was the closest to the interface, with the change in depth between the steps set to 0.25 mm.

Following the above preparation procedure, a specially designed shear fixture mounted in an Instron testing machine was used to fracture, in turn, the five shallowest steps. Failure of the step was deemed to occur at the point of maximum load for the step. Because the sixth step was located well within the relatively strong copper, attempts at its removal resulted in significant distortion of the samples and thus introduced doubts as to the validity of the values

obtained for this step. For this reason, the sixth step was left largely untouched. Both sides of the removed steps were kept for future examination, both by scanning electron microscopy (SEM) and by cross-sectional optical metallography, to determine the fracture path and the mode of fracture.

Measurement of the growth kinetics of the intermetallic layers was also undertaken. For each of the treatment conditions ten samples were cut from the unused end portions of the mechanical testing samples. These were then mounted in cross-section in cold-mounting resins and prepared for optical examination. A representative micrograph was taken of the interfacial region for each of the prepared samples, and 50 measurements were then made of each phase along the copper/solder interface. The reported thickness values were the mean value of these measurements.

For X-ray determinations, copper bars, 76.2 mm by 15.2 mm, were cut from the stock sheet. The pre-treatment preparation of these samples was the same as that used for the mechanical testing samples. The solder for these tests was prepared by rolling the stock material into a strip nominally 0.50 mm thick, from which rectangles of 9.6 mm by 19.1 mm were cut. The samples were stacked in a three-tiered sandwich structure (Fig. 1b), and heat treated according to the previously used schedule. Following air cooling, the samples were broken by pulling apart components 2 and 3 of Fig. 1b, and the fracture surfaces scanned using  $\text{CuK}\alpha$  radiation in a Rigaku  $2\theta/\theta$  analyser. Analysis of the recorded scans was performed to identify the intermetallic phases present as a function of time and temperature.

### 3. Results and discussion

#### 3.1. X-ray diffraction

The manner in which the samples for the X-ray analysis were prepared was selected in order to provide two fracture surfaces for examination for each of the treatment conditions. This was the case at 300 and 350°C, where the samples were observed to fail in a very brittle manner. At 230°C, however, considerable ductility was encountered during the fracture process, resulting in the loss of one of the faces to extreme curvature.

The scans obtained were indexed using the results of Tu [6]. In all cases the peaks could be indexed completely as  $\text{Cu}_6\text{Sn}_5$  ( $\eta$ ),  $\text{Cu}_3\text{Sn}$  ( $\epsilon$ ), Cu, Pb and Sn, although these latter two appeared in very few cases. The peaks used for identification of the intermetallics are shown in Table I and were the dominant ones in most samples. For all samples for which two faces were available for examination, different peaks were found on either face. Fig. 2 shows X-ray scans for the two faces obtained for one of the samples. One face exhibited almost completely  $\text{Cu}_6\text{Sn}_5$  peaks, while the other resulted in the appearance of a combination of  $\text{Cu}_6\text{Sn}_5$  peaks and  $\text{Cu}_3\text{Sn}$  peaks. This suggests that the failure has occurred within the intermetallic layer, and moreover, apparently, within the  $\text{Cu}_6\text{Sn}_5$  layer itself. Microscopic examination of both fracture surfaces revealed that the fracture was brittle and intergranular, and thus had likely occurred at some point within the

TABLE I Major peaks used for intermetallic identification

| Temperature (°C) | Time (min) | $\eta$ -(101) | $\eta$ -(002) | $\epsilon$ -(200) | $\epsilon$ -(002) |
|------------------|------------|---------------|---------------|-------------------|-------------------|
| 230              | 30         | P             | A             | P                 | A                 |
|                  | 60         | P             | P             | P                 | A                 |
|                  | 90         | P             | A             | A                 | A                 |
|                  | 120        | P             | P             | A                 | A                 |
|                  | 150        | P             | P             | P                 | A                 |
|                  | 180        | P             | P             | A                 | A                 |
| 300              | 30*        | P             | P             | A                 | P                 |
|                  | 60*        | P             | P             | A                 | P                 |
|                  | 90*        | P             | P             | P                 | P                 |
|                  | 120*       | P             | P             | A                 | P                 |
|                  | 150*       | P             | P             | A                 | P                 |
|                  | 180*       | A             | P             | P                 | P                 |
| 350              | 30*        | P             | P             | A                 | A                 |
|                  | 60*        | P             | P             | P                 | P                 |
|                  | 90*        | P             | P             | P                 | P                 |
|                  | 120*       | P             | P             | P                 | P                 |

Notes:  $\eta = \text{Cu}_6\text{Sn}_5$ .  $\epsilon = \text{Cu}_3\text{Sn}$ .

P = peak was present, A = peak was absent.

Those tests marked with an asterisk indicate situations in which two faces were available for examination.

intermetallic region. As will be seen later, this corresponds to the same pattern for failure found in the mechanical samples and thus provides support for the results of the mechanical tests.

#### 3.2. Mechanical properties

During removal of the steps, it was observed that failure of the interfacial step occurred in two stages. Fracture of the step initiated in the intermetallic layer and was characterized by a sharp load-extension curve, typical of a brittle material. This can be seen in Fig. 3, where the curve for the interfacial step is labelled 4, and corresponds to the step labelled 4 in Fig. 1a. This mode of failure accounted for separation of only part of the step, as a remaining ligament of solder had to be traversed in order to achieve complete removal of the step. This two-step fracture was observed for all of the samples.

Following machining of the samples, it was noticed that in some cases there was a significant amount of macroscopic porosity. In the instances where this occurred at the interfacial step, the samples could not be used, and thus some of the samples were rejected and a number less than seven was used for the tests. The number of samples used was, however, never less than four. The mean values for the bond strength at 230, 300 and 350°C are shown in Fig. 4. As can be seen, the values for the strength range between 92 and 55 MPa. These values are significantly higher than previously reported values of between 20 and 40 MPa for similar testing conditions [1–3]. The considerable scatter obtained in the present results is attributable to a combination of experimental difficulties and, more importantly, a varying and undetected degree of microporosity in some specimens. Statistical analysis of the data was therefore conducted to determine if any significant changes in the value of the strength could be deduced as a function of time for any given temperature. A summary of the statistical study is presented in Table II. Using a standard student's *t*-test

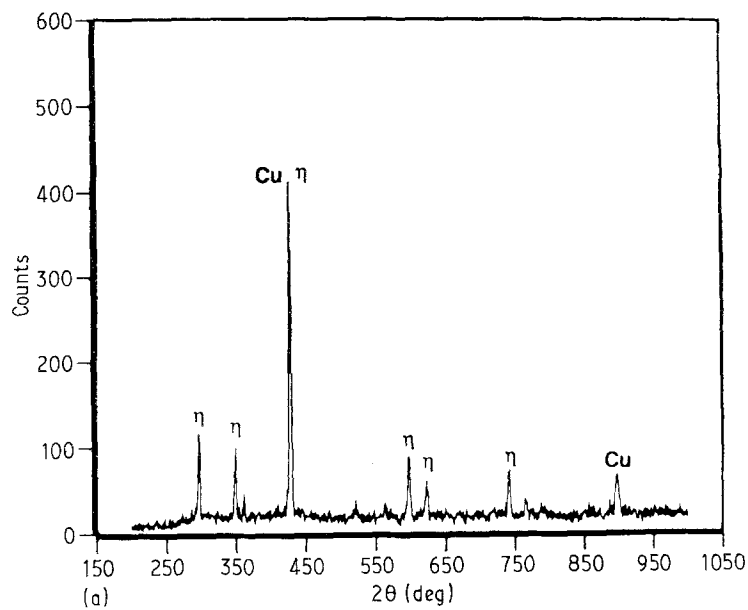
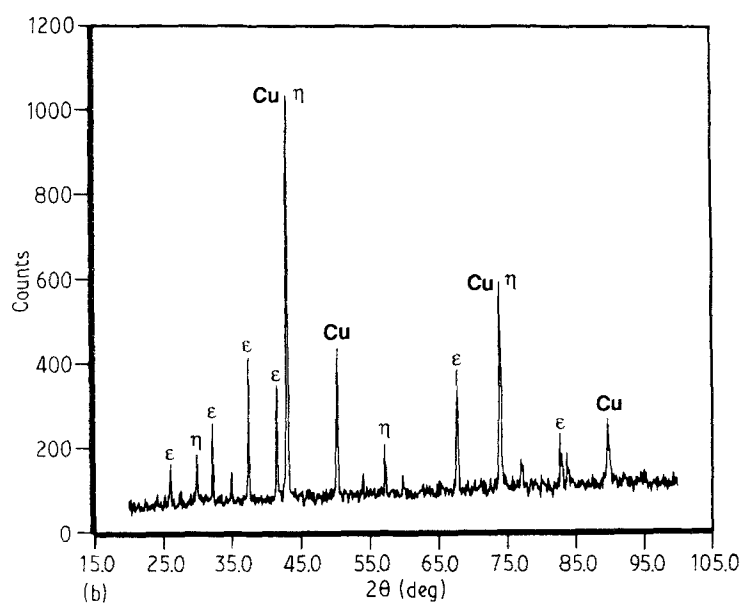


Figure 2 X-ray scans of both surfaces obtained for the sample formed at 350°C for 60 min: (a) fracture surface showing Cu and Cu<sub>6</sub>Sn<sub>5</sub> ( $\eta$ ) peaks only; (b) fracture surface showing additional Cu<sub>3</sub>Sn ( $\epsilon$ ) peaks.



at a 95% confidence level, it was found that at 300 and 350°C any observed changes occurring in the strength were the result of statistical variations in the values obtained. However, at 230°C there was a significant increase in the strength from 5 to 60 min, with no

TABLE II Summary of statistics for bond strength evaluations

| Temperature (°C) | Time (min) | Mean (MPa) | S.D. (MPa) |
|------------------|------------|------------|------------|
| 230              | 5          | 65.8       | 1.5        |
|                  | 30         | 80.2       | 6.4        |
|                  | 60         | 91.5       | 9.3        |
|                  | 90         | 55.3       | 2.9        |
|                  | 120        | 69.6       | 4.6        |
|                  | 150        | 65.7       | 7.0        |
|                  | 180        | 82.5       | 4.7        |
| 300              | 5          | 60.6       | 8.0        |
|                  | 30         | 64.0       | 8.7        |
|                  | 60         | 54.1       | 10.6       |
|                  | 90         | 61.3       | 15.5       |
|                  | 120        | 72.3       | 12.0       |
|                  | 150        | 63.6       | 19.5       |
|                  | 180        | 71.5       | 6.5        |
| 350              | 5          | 58.5       | 6.3        |
|                  | 30         | 60.5       | 13.6       |
|                  | 60         | 70.2       | 12.2       |
|                  | 90         | 67.8       | 9.8        |
|                  | 120        | 58.1       | 19.4       |

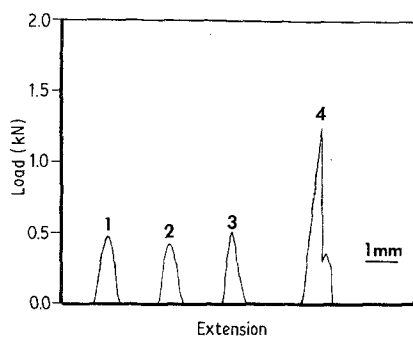


Figure 3 Typical load-extension curve for the strength test. The numbers correspond to step numbers from Fig. 1a. Peaks 1, 2 and 3 represent the deformation behaviour of steps completely within the solder.

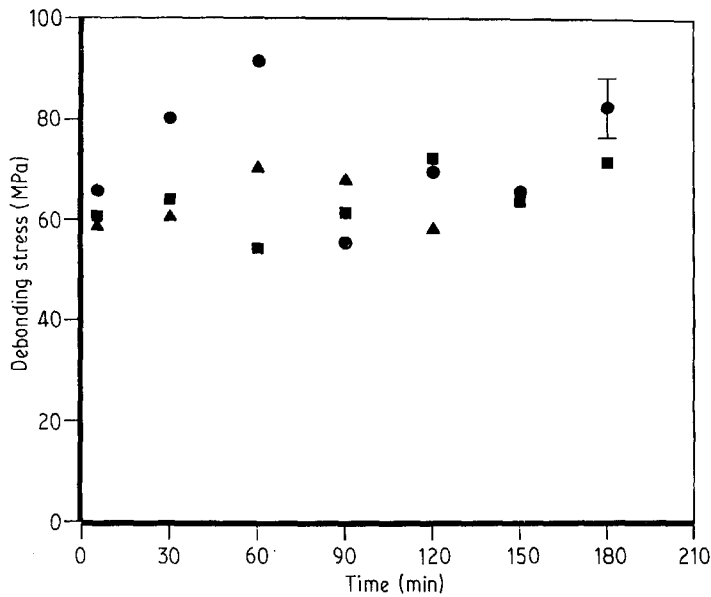


Figure 4 Stress-to-failure values of the copper/solder bond for (●) 230, (■) 300 and (▲) 350° C.

notable change occurring between 60 and 180 min. The drop in strength which occurred at 90 min, and was also evident at 120 and 150 min, appears to have been the result of some unidentified experimental or physical effect. It was surprising as there was no difference in the manner in which the step was removed in these samples of low debonding stress and the others at 230° C, nor was there any indication of a serious degradation in the quality of the bond in these instances.

Statistical analysis was also performed to investigate changes in the strength with temperature. Between 300 and 350° C, the differences were found to be statistically insignificant, with the two temperatures sharing equally the incidences of having the higher value. Between 230 and 300° C, however, the differences in strength at 30, 60 and 180 min were found to have significance, and were more pronounced at the lower times. The strength of the interface thus appears to reach a minimum value for temperatures greater than 300° C.

A microscopic examination of the interfacial region reveals the expected two layers between the copper

and the solder, as can be seen in Fig. 5. The larger, lighter region has been identified in previous work [1, 2, 9] as  $\text{Cu}_6\text{Sn}_5$  ( $\eta$ ), and the thinner grey region as  $\text{Cu}_3\text{Sn}$  ( $\epsilon$ ). It is within the former phase that fracture is believed initially to occur. In support, Fig. 6 shows scanning electron micrograph for the removed part of the interfacial step for the sample formed at 300° C for 120 min. The fracture at the leading edge of the step clearly appears brittle in nature. The dual nature of the fracture surface may also be seen, with varying portions of the step showing a tearing morphology, indicative of the secondary ductile fracture associated with the solder. Fig. 7, taken from the brittle part of the fracture surface, reveals that the brittle fracture is in fact intergranular, suggesting that the intermetallic layers grow in a polycrystalline rather than monolithic manner. This agrees with previous observations of this aspect of the structure of such intermetallic layers [6].

Fig. 8 shows an example of a sample prior to complete failure of the interfacial step. It is evident from this that the crack has passed through the intermetallic layer, and not along the intermetallic/solder

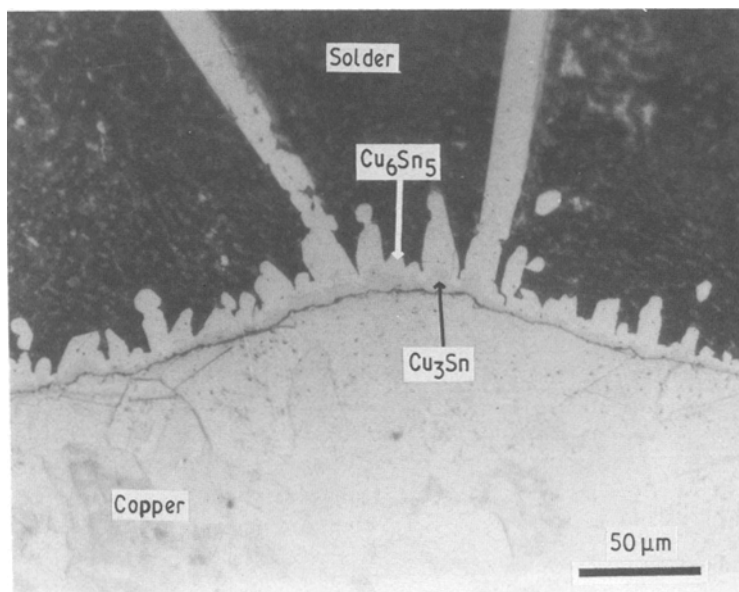


Figure 5 Cross-section of the joint formed at 350° C for 120 min showing both intermetallic layers:  $\text{Cu}_6\text{Sn}_5$  (light region immediately below solder) and  $\text{Cu}_3\text{Sn}$  (light grey region between copper and  $\text{Cu}_6\text{Sn}_5$ ).

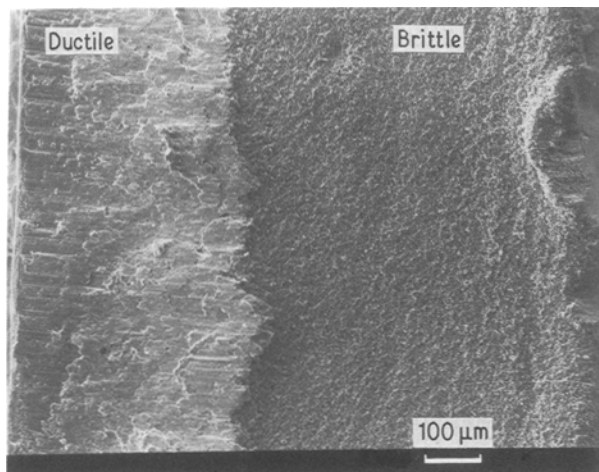


Figure 6 Scanning electron micrograph of the fracture surface for the joint formed at 300°C for 120 min, showing the dual nature of the failure of the step.

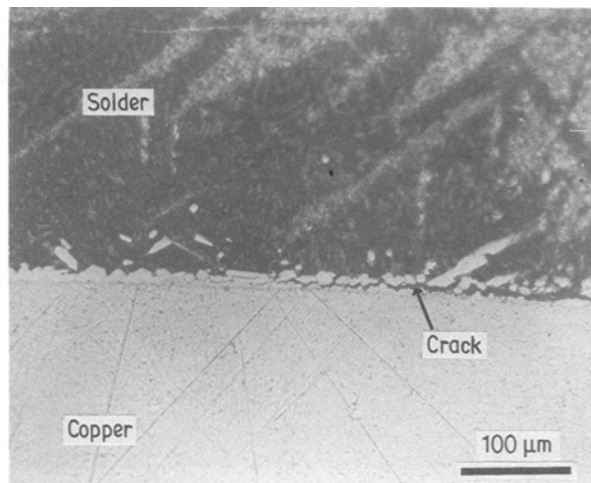


Figure 8 Cross-sectional view of the interface of the sample formed at 350°C for 90 min, showing the crack running through the  $\text{Cu}_6\text{Sn}_5$  layer.

boundary, as had been reported in previous studies [1–3]. This behaviour was found to exist in all the samples analysed, even at the lowest time and temperature, although in a few instances, notably at 300 and 350°C, the crack was seen to travel for short distances along the  $\eta/\epsilon$  boundary. Fig. 9 shows scanning electron micrographs for the fracture surfaces from the copper side of the interfacial step for 230 and 300°C. It can be seen that the area of the fracture surface characterized as intergranular increases with increasing temperature. The implications of all of these latter observations will be considered later in light of the results obtained for the thickness measurements.

### 3.3. Growth study

Representative micrographs of the cross-sections used for growth measurements are shown in Fig. 10. It can be seen that the  $\text{Cu}_6\text{Sn}_5$  grows in a very irregular manner, consisting of a series of saw-toothed protrusions which became more pronounced with increasing time and temperature. The average results for measurements of  $\text{Cu}_6\text{Sn}_5$  obtained for all three temperatures

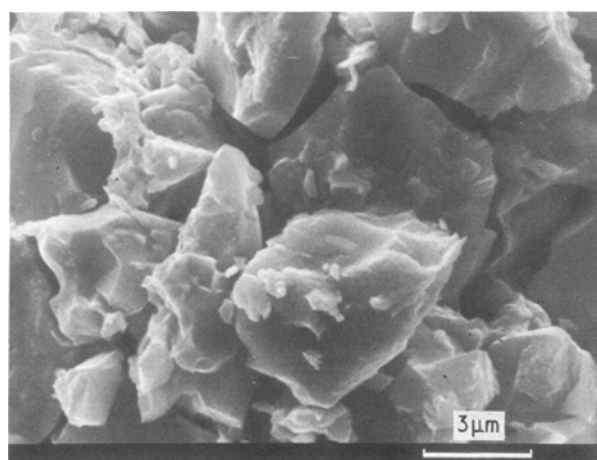


Figure 7 Scanning electron micrograph of the brittle region of the joint formed at 300°C for 180 min, showing the intergranular nature of the fracture.

are shown in Fig. 11. Statistical analysis of the data indicated the lack of any trend with time beyond 30 min, suggesting the possibility that most of the growth occurs within the first 30 min, with subsequent increases being too small to detect with the measurement technique used. This apparent limit to the growth has been observed in similar systems [16] and was described as being the result of the competition between the motion of the intermetallic/metal interface and dissolution occurring at the intermetallic/liquid boundary, evidence for the dissolution phenomenon residing with the observed faceting of the intermetallics [16, 17]. This faceting was seen in some of the samples in this work, and thus the lack of increase with time may be a result of competition between the motion of the  $\text{Cu}_3\text{Sn}/\text{Cu}_6\text{Sn}_5$  boundary and some dissolution of the  $\text{Cu}_6\text{Sn}_5$  into the liquid solder. Alternatively, the bulk of the growth after 30 min may have been incorporated in the extension of the extreme growth points, with the remainder of the layer remaining relatively static.

It is apparent from Fig. 11 that the greatest change in thickness occurs between 230 and 300°C. Past 30 min, the thickness increases from approximately 6  $\mu\text{m}$  to about 15  $\mu\text{m}$  between these two temperatures. Apart from the anticipated increase in kinetics resulting from increased diffusion at the higher temperatures, an additional explanation for the increase arises from consideration of the phase diagrams. At 230°C, the solubility of copper in both lead and tin is negligible, and thus saturation of the liquid solder might be expected to occur fairly rapidly, especially in light of the fact that copper dissolves rapidly in molten solder [11]. This saturation may limit the motion of the  $\text{Cu}_6\text{Sn}_5$ . For the higher temperatures, the solubility of copper in tin increases to approximately 96.5 to 97.5% (for 300 and 350°C, respectively). This would delay the retarding action of saturation of the solder melt, and thus could partially account for the increased thickness of  $\text{Cu}_6\text{Sn}_5$  at the higher temperatures. The similarity in the solubility limits for 300 and 350°C also helps to explain the smaller change in

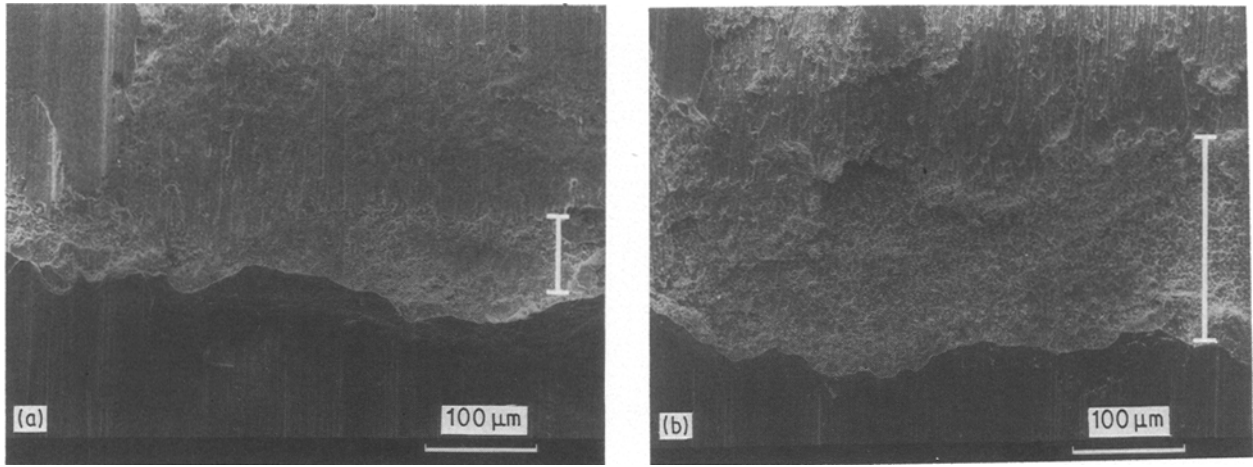


Figure 9 Scanning electron micrographs showing the extent of the brittle region occupying the fracture surface, as indicated by the bars to the side of the pictures for (a) the sample formed at 230°C for 30 min, and (b) the sample formed at 350°C for 120 min.

thickness occurring between these two temperatures, as compared to that between 230 and 300°C.

The variation of mean values of thickness with time for the  $\text{Cu}_3\text{Sn}$  layer is shown in Fig. 12. Changes in thickness with temperature parallel the pattern observed with  $\text{Cu}_6\text{Sn}_5$ , with most of the change occurring between 230 and 300°C, especially at longer times. Statistical analysis revealed that  $\epsilon$  grows linearly with time, with a slope whose value increases from  $0.00347 \mu\text{m min}^{-1}$  at 230°C to  $0.0146 \mu\text{m min}^{-1}$

at 350°C, values of the same order of magnitude as those encountered previously [4]. This linear behaviour suggests that the growth of  $\epsilon$  is controlled by some type of interfacial reaction, rather than by the long-range diffusion of either copper or tin. It should also be noted that the difference between successive slopes decreases with increasing temperature, indicating that there may again be some limit to the rate of change once a sufficiently high temperature is reached.

As discussed previously, the role of changing thickness in establishing the strength of the interface has previously been treated in an empirical manner. It has simply been stated that decreases in the strength are accompanied by increases in the size of the intermetallic layers [1, 2]. This pattern was again observed here, where the decrease in strength from 230 to 300°C was accompanied by the observed increase in the thickness of  $\text{Cu}_6\text{Sn}_5$  between the two temperatures. Also, the similarity in the thickness values for the two higher temperatures accounts for the lack of difference in the value obtained for the bond strength in these two cases.

It was found that the failure of all steps originated in the  $\text{Cu}_6\text{Sn}_5$  layer. Values of the strength of the bond

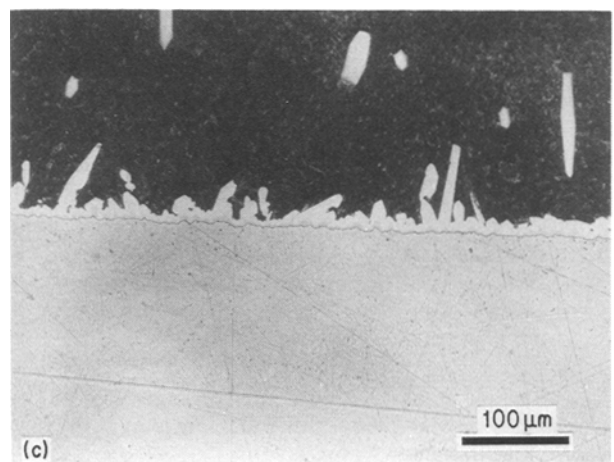
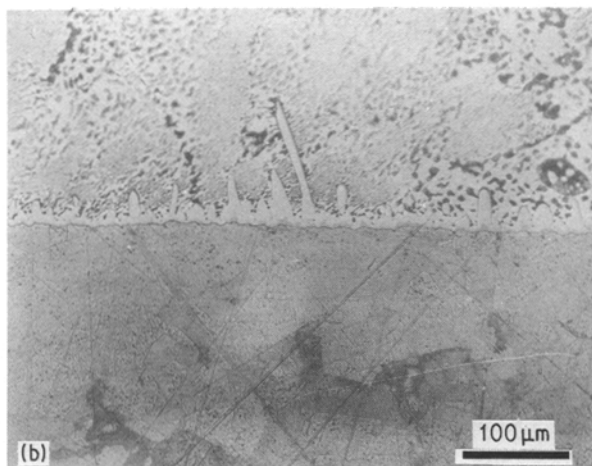
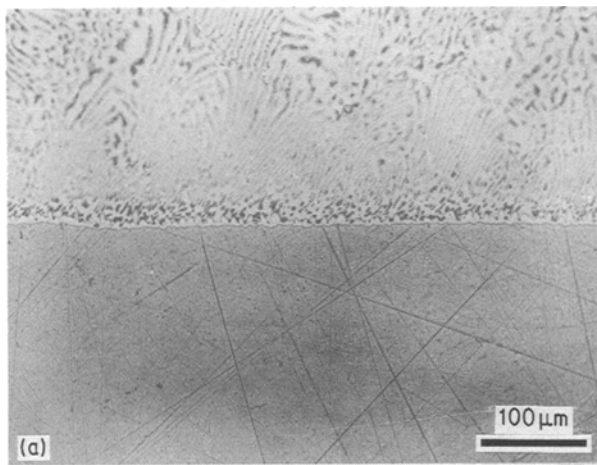


Figure 10 Examples of cross-sections used for intermetallic thickness measurements: samples prepared at (a) 230°C for 60 min, (b) 300°C for 60 min, and (c) 350°C for 60 min.

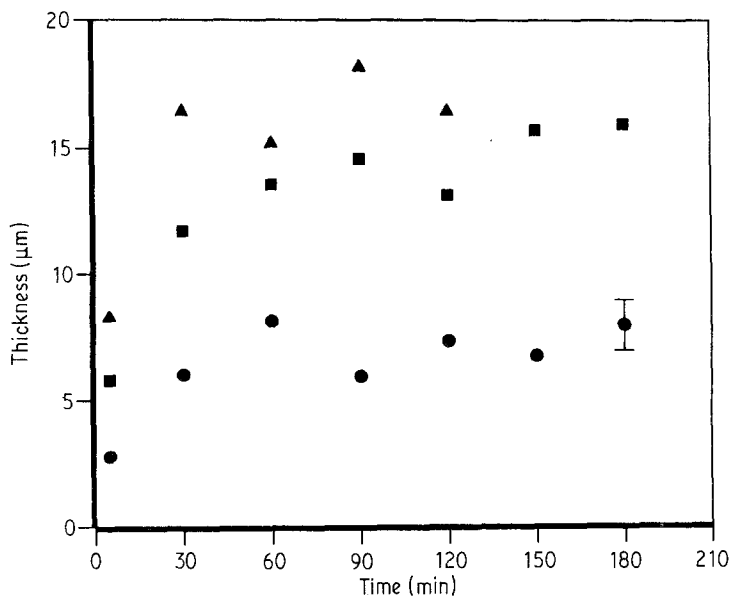


Figure 11 Thickness of  $\text{Cu}_6\text{Sn}_5$  as a function of time for (●) 230, (■) 300 and (▲) 350°C.

might thus be expected to correspond to the value of the strength of the intermetallic itself for this mode of deformation, and thus might well be expected to be the same for all cases, regardless of changes in thickness. For  $\text{Cu}_6\text{Sn}_5$  thicknesses greater than  $10\ \mu\text{m}$ , this does indeed seem to be the case. For the tests performed at  $230^\circ\text{C}$ , it is not clear what the precise explanation for the apparent increase in strength might be, though the following is presented as a possible explanation: increased strength of soldered or brazed joints has been observed in instances where the solder or braze is weaker than and in smaller quantities than the base metal. In that case, the solder or braze was constrained from deforming and a hydrostatic stress state was induced in the solder or braze, resulting in an increase in the strength of the joint [18–20]. In the present situation, the copper was found to be stronger than the  $\text{Cu}_6\text{Sn}_5$ , and the ratio of copper thickness to  $\eta$  thickness was of the order 200:1. As the size of the intermetallic layer decreased, more of the applied stress should be transferred to the copper, and the overall level of stress required to initiate failure within

the intermetallic would then be increased. This effect would, however, be limited to intermetallic layer thicknesses greater than  $5\ \mu\text{m}$ .

The increase in the fracture surface area covered by intergranular fracture is also related to the increasing thickness of the  $\text{Cu}_6\text{Sn}_5$  layer. Fig. 8 shows a crack running through the  $\text{Cu}_6\text{Sn}_5$  with an irregular path, typical of an intergranular fracture. At some point the travelling crack should branch up into the solder above the layer, and in this ductile phase the crack would then be considerably slowed or even stopped. As the thickness of the intermetallic increases the crack path is expected to have a longer residence time within the  $\text{Cu}_6\text{Sn}_5$  before branching into the solder. Thus, larger areas of the joint would fail in this manner with increasing temperature, once the requisite value of stress for failure initiation is reached. This effect can be observed in Fig. 9a and b, where the extent of brittle failure at  $350^\circ\text{C}$  is much larger than at  $230^\circ\text{C}$ , exactly as would be expected because of the greater size of the intermetallic layer at  $350^\circ\text{C}$ . Comparison of the fracture surfaces between 300 and

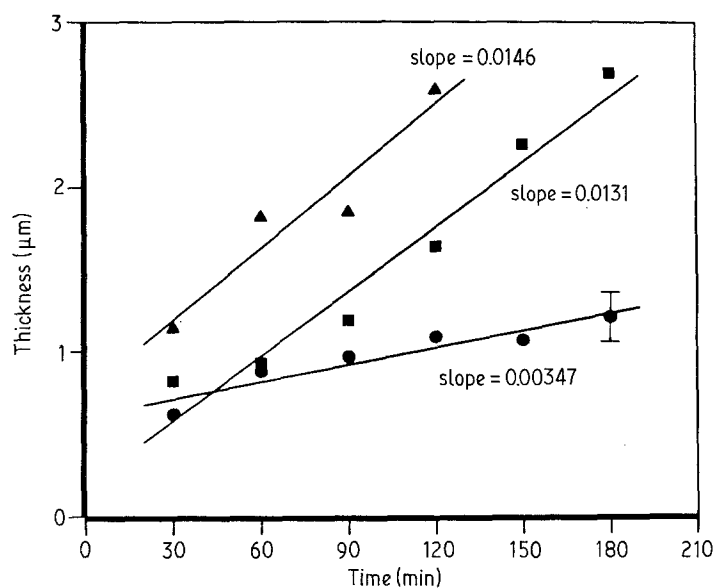


Figure 12 Thickness of  $\text{Cu}_3\text{Sn}$  as a function of time for (●) 230, (■) 300 and (▲) 350°C.



350°C indicated little difference in the extent of the region of brittle failure, as might be expected from the similarity in the values obtained for the thickness of the Cu<sub>6</sub>Sn<sub>5</sub>.

For the Cu<sub>3</sub>Sn layer, there was no indication that increases in its thickness affected the strength or extent of brittle failure in any of the samples. There were some isolated instances of the crack following the Cu<sub>3</sub>Sn/Cu<sub>6</sub>Sn<sub>5</sub> interface, but there was no occasion where the crack followed this path exclusively. It appears, then, that this boundary does not represent a significantly weak point in the joint region, and indications are that the Cu<sub>3</sub>Sn layer also does not provide an alternate path for the crack. The role of this phase in determining the strength of the interfacial bond thus appears to be indirect at best, inasmuch as it may limit the growth of Cu<sub>6</sub>Sn<sub>5</sub>.

#### 4. Conclusions

1. The presence of both Cu<sub>6</sub>Sn<sub>5</sub> and Cu<sub>3</sub>Sn was confirmed by X-ray diffraction for all times and temperatures considered.

2. The strength of the bond at the interface reached a maximum of 91.5 MPa for 60 min at 230°C, then dropped to a minimum value of roughly 60 MPa for temperatures greater than 300°C. The strength generally showed no change with time beyond 30 min.

3. Failure began in the Cu<sub>6</sub>Sn<sub>5</sub> layer in all cases, then branched into the solder after a period of travel. The extent of failure within the Cu<sub>6</sub>Sn<sub>5</sub> increased with increasing temperature, and was a result of the concomitant increase in the thickness of the combined intermetallic layer.

4. The thickness of Cu<sub>6</sub>Sn<sub>5</sub> reached a limiting value after 30 min for all temperatures. The thickness increased dramatically from 6 μm at 230°C to 15 μm at 300°C, much less so from 300 to 350°C. The thickness of Cu<sub>6</sub>Sn<sub>5</sub> played the greatest role in determining the strength of the bond, as changes in the strength reflected more closely changes in the thickness of this layer.

5. Cu<sub>3</sub>Sn grew linearly with time for the times investigated, with the rate of growth increasing from 0.00347 μm min<sup>-1</sup> at 230°C to 0.0146 μm min<sup>-1</sup> at 350°C. As in the case of Cu<sub>6</sub>Sn<sub>5</sub> the thickness increased with temperature, with no apparent limit to the increase. The presence of a Cu<sub>3</sub>Sn layer was not significantly involved in determining the strength of the interfacial bond.

#### Acknowledgements

Support from the Center for the Study of Materials, through the Materials Research Laboratory section, National Science Foundation, under grant number DMR 8521805 is gratefully acknowledged. The X-ray diffraction equipment, provided by the Division of Materials Research of the National Science Foundation under grant number DMR 8005380, was essential for this work. Thanks are extended to various faculty staff and students at Carnegie Mellon University for their suggestions and support during the course of the research.

#### References

1. R. A. HAGSTROM and R. N. WILD, in Proceedings of the Technical Programme, International NEPCON (National Electronic Packaging and Production Conference), Brighton, October 1969, (Kiver, Communications Inc.) p. 271.
2. K. R. STONE, R. DUCKETT, S. MUCKETT and M. WARWICK, *Brazing Soldering* No. 4 (1983) 20.
3. W. J. TOMLINSON and N. J. BRYAN, *J. Mater. Sci.* **21** (1986) 103.
4. S. J. MUCKETT, M. E. WARWICK and P. E. DAVIS, *Plating Surf. Finishing* **79** (1986) 44.
5. H. N. KELLER and J. M. MORABITO, *Surf. Interface Anal.* **3** (1981) 16.
6. K. N. TU, *Acta Metall.* **21** (1973) 347.
7. P. W. DEHAVEN, G. A. WALKER and N. A. O'NEIL, *Adv. X-Ray Anal.* **27** (1983).
8. H. BERG and E. L. HALL, in Proceedings of 11th Annual Conference on Reliability Physics, Las Vegas, 3-5 April 1973 (IEEE, New York, 1973) p. 10.
9. W. G. BADER, *Welding J.* **48** (1969) 551-s.
10. "Metals Handbook" Vol. 8, 8th Edn (American Society for Metals, Metals Park, Ohio, 1973) p. 251-338.
11. C. J. THWAITES, *Int. Met. Rev.* **17** (1972) 149.
12. W. J. REICHENECKER, *Tin and Its Uses* No. 130 (1981) 14.
13. K. N. TU and R. D. THOMPSON, *Acta Metall.* **30** (1982) 947.
14. P. W. DEHAVEN, IBM Internal Report IBM-EF-52 (1984).
15. R. BLICKENSERFER and J. M. BURRUS, *J. Test. Eval.* **12** (1984) 3.
16. S. K. KANG and V. RAMACHANDRAN, *Scripta Metall.* **14** (1980) 421.
17. H. FIDOS and M. SCHREINER, *Z. Metallkde* **61** (1970) 225.
18. W. G. MOFFATT and J. WULFF, *Welding J.* **42** (1963) 115-s.
19. H. P. MEISSNER and G. H. BALDAUF, *Trans. ASME* **73** (1951) 697.
20. C. W. SHAW, L. A. SHEPARD and J. WULFF, *ibid.* **57** (1964) 94.

Received 27 July

and accepted 23 October 1987